

## MICROSTRUCTURAL EVOLUTION AND MECHANICAL PERFORMANCE OF RESISTANCE SPOT WELDED DP1000 STEEL WITH SINGLE AND DOUBLE PULSE WELDING

CHABOK Ali<sup>1</sup>, VAN DER AA Ellen<sup>2</sup>, DE HOSSON Jeff<sup>3</sup>, PEI Yutao<sup>1</sup>

<sup>1</sup> *Department of Advanced Production Engineering, Engineering and Technology Institute Groningen, University of Groningen, the Netherlands*

<sup>2</sup> *Tata Steel, IJmuiden, the Netherlands*

<sup>3</sup> *Department of Applied Physics, Zernike Institute for Advanced Materials, University of Groningen, Groningen, The Netherlands*

### Abstract

Two welding schemes of single and double pulse were used for the resistance spot welding of DP1000 dual phase steel. The changes in the mechanical performance and variant pairing of martensite under two different welding conditions were scrutinized. It is demonstrated that, although both welds fail in pull-out failure mode, double pulse welding enhances cross-tension strength and energy absorption capability of the weld compared to single pulse welding process. Double pulse welding effectively changes the microstructure of the fusion zone. While the fusion zone of single pulse welds has a typical microstructure of columnar grains, the initial fusion zone of double pulse welds is subdivided into two zones: the outer recrystallized layer composing of martensitic microstructure formed within the equiaxed prior austenite grains, and the inner part of columnar grains resulted from the rapid solidification process of resistance spot welding. Orientation imaging microscopy results show that the recrystallized layer of double pulse welds exhibits a lower fraction of high-angle grain boundaries and coarse structure of Bain groups.

**Keywords:** Dual phase steel, resistance spot welding, cross-tension test, orientation imaging microscopy

### 1. INTRODUCTION

Advanced high strength steels (AHSS) including dual phase (DP) steels belong to a new generation of steels which are extensively used in automotive industries to design the car body structure. Their use has been readily increasing over the years, mainly because of their mechanical performance offering both high strength and good formability. They provide a group of advanced engineering materials for next reduction of car body weight in order to enhance fuel economy without compromising on safety. Dual phase (DP) steels with a microstructure consisting of martensite and ferrite are commonly used for safety parts in car bodies, e.g. bumpers, and side impact beams etc. [1].

Resistance spot welding (RSW) is the predominant joining technique in automobile body production with a typical vehicle containing 4000 ~ 5000 spot welds. However, it has been reported that for AHSS of strength > 800 MPa, the cross-tension strength of the RSW joints tends to decrease with increasing tensile strength of the base material [2]. This is due to the relatively high level of alloying elements in combination with an increasing stress concentration at the weld nugget circumference during loading. Higher hardenability of these steels combined with the ultra-fast cooling cycle of RSW may lead easily to the formation of martensitic microstructure with higher brittleness. Due to lower fracture toughness of nugget, crack can easily propagate through the weld causing brittle fracture during cross-tension test [3-5].

In this investigation, single and double pulsed schemes were applied in order to study the change in the mechanical properties and microstructural evaluation of resistance spot welded DP1000 steel. The effects on the mechanical properties were studied using cross-tension tests and Vickers hardness measurement. Furthermore, orientation imaging microscopy (OIM) was used to investigate the crystallographic features of the formed martensite and their effect on the mechanical performance of the weld.

## 2. EXPERIMENTAL

The material examined was dual phase 1 GPa (PD1000) AHSS sheet of 1.5 mm thickness. In order to study the effect of welding scheme on the microstructural and mechanical characteristics of the welds, two welding schedules, a single and double pulse weld schemes, were applied. **Figure 1** shows a scheme of the welding schedules for single and double pulse processes.

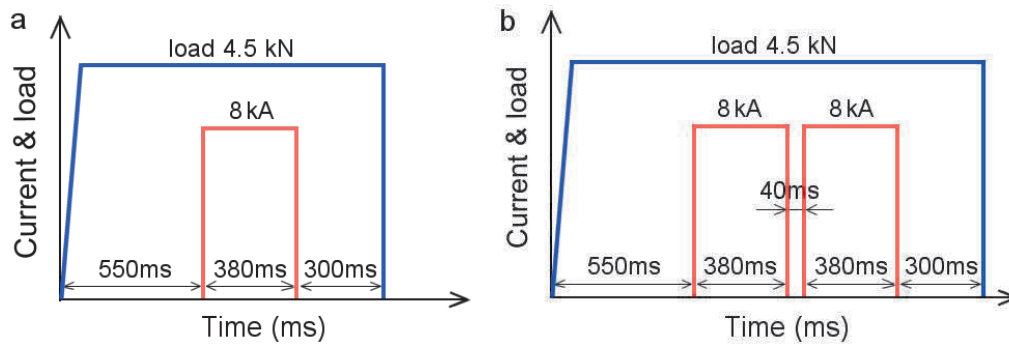


**Figure 1** RSW scheme for single pulse weld (a) and double pulse weld (b)

The OIM characterization was carried out by electron back scatter diffraction pattern using a Philips ESEM-XL30 scanning electron microscope equipped with a field emission gun operating at 20 kV.

Vickers micro-hardness measurements were performed at 200 g load for a loading time of 15 s. In order to evaluate the mechanical performance of the welds produced by different welding scheme, cross-tension tests were performed for both single and double pulse welds (150 × 50 mm samples).

## 3. RESULTS AND DISCUSSION

**Figure 2** depicts representative load-displacement curves of single and double pulse welds. Double pulse welds exhibit better mechanical performance as the average maximum load increases from 9.2 kN for single pulse weld to 11.7 kN for double pulse weld. Moreover, the average energy absorption rises from 55.3 J for single pulse welds to 75.2 J for double pulse welds.

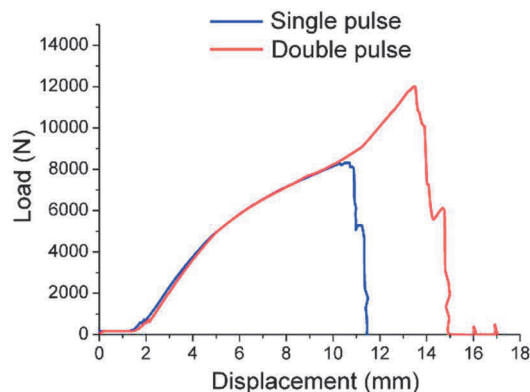


**Figure 2** Representative load-displacement curve of single and double pulse welds in cross-tension test

The nugget size of both welds is ~7 mm, ruling out possible effect of the weld size on the mechanical behaviour of the welds. Cross sections of fractured samples after cross-tension test are shown in **Figure 3**, together with an insert, indicating the fracture path of the welds. It should be noted that a single pulse weld shows a typical fusion zone (FZ) microstructure with columnar grains resulting from the rapid solidification process of the RSW.

In the case of double pulse weld, the initial FZ structure of the first pulse is subdivided into two zones: the inner part composed of columnar grains, and the outer layer that has an equiaxed microstructure. The dashed lines in **Figure 3b** indicate the boundaries of the inner part and outer layer. In the case of the single pulse welds, failure occurs at the coarse grain heat affect zone (CG-HAZ) adjacent to the FZ. On the contrary, two failure zones are associated with the double pulse welds. On the left side, failure occurs close to the weld nugget as the crack penetrates a small distance in the Rex-zone and then is redirected towards the sheet thickness. On the right side, fracture originates at sub-critical heat affected zone (SC-HAZ), outside the weld nugget and close to the base metal leading to creating a lip.

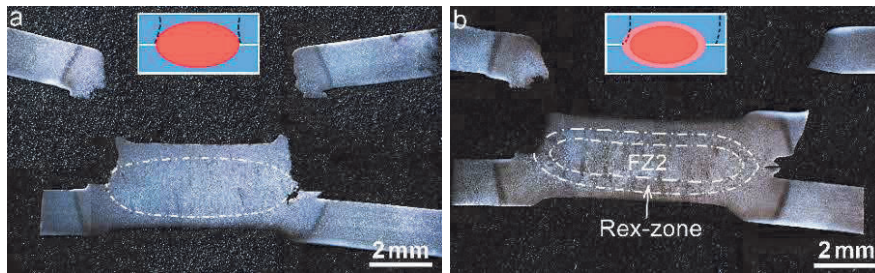


**Figure 3** Cross sectional view of cross-tension tested single pulse weld (a) and double pulse weld (b) with an insert schematically showing the fracture path

**Figure 4** depicts the measured Vickers hardness distribution across the different microstructural zones of the welds. As illustrated, there is no big difference between the hardness of FZ for the single pulse weld and FZ2 of double pulse weld. However, the Rex-zone of double pulse weld shows significant reduction in hardness compared to its corresponding area in the single pulse weld. Another characteristic of hardness distribution is that both welds show softening in the SC-HAZ with respect to the base metal with the hardness value of 303 HV. Obviously, the degree of softening is more pronounced for the double pulse weld, with a minimum hardness level 260 HV versus 281 HV in the SC-HAZ of the single pulse weld.

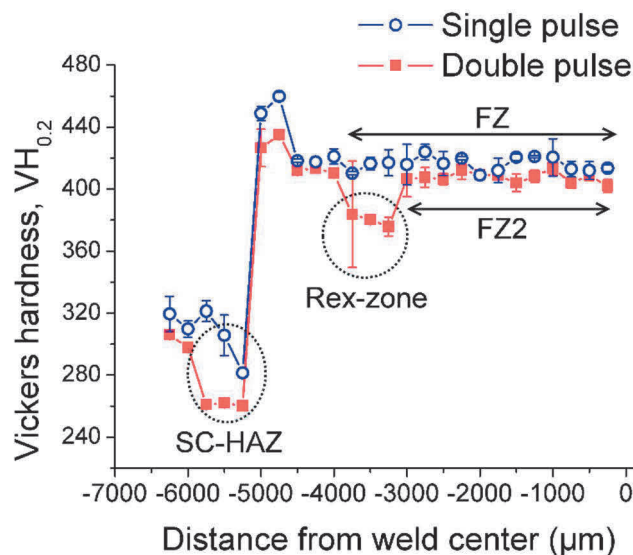


**Figure 4** Microhardness profile of the single and double pulse welds

**Figure 5a** and **5b** depict the corresponding kernel average misorientation (KAM) maps of the two welds. The local residual strain could be safely explained by KAM map as an increase in the strain leads to an increase in the local lattice rotation. As illustrated in **Figure 5a**, the KAM value for single pulse weld decreases with moving over CG-HAZ towards FZ, and then increases again in the FZ. For double pulse welds, the lowest

KAM values are achieved in the Rex-zone (**Figure 5b**). Thus the FZ2 with a higher residual strain is surrounded by a recrystallized shell that has a lower residual strain. For both samples, the outer CG-HAZ far from the nugget shows the highest KAM value that indicates the highest residual strain.

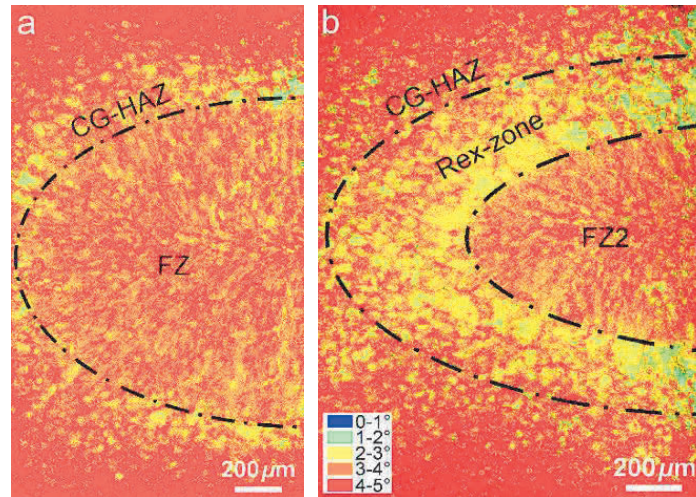


**Figure 5** Kernel average misorientation map of single (a) and double (b) pulse weld

The fracture toughness of martensitic microstructure is strongly affected by its resistance to transgranular fracture as the main fracture mode in lath martensite [6]. Transgranular fracture results from rapid propagation of crack along a particular crystallographic plane [7]. For high strength steels with a BCC structure cleavage fracture occurs on {100} planes [6]. It was reported that high density of high-angle grain boundaries with misorientation larger than 45° enhances the toughness of HAZ of low carbon steel [8].

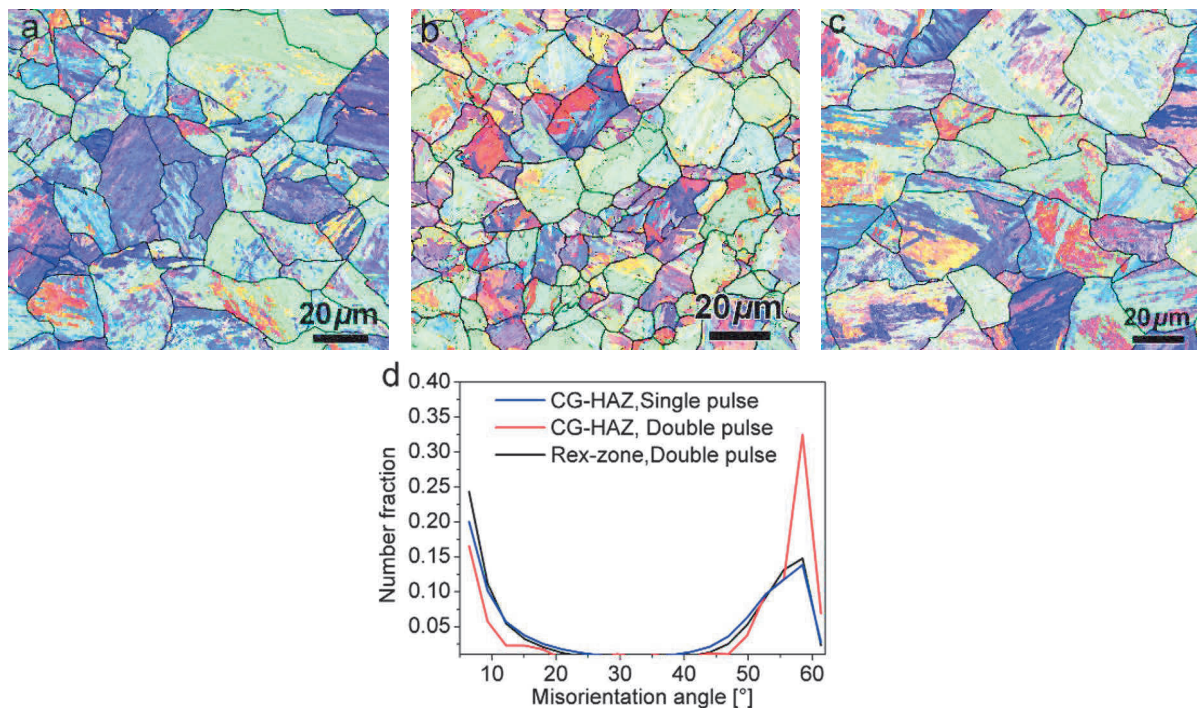


**Figure 6** Inverse pole figure maps of CG-HAZ of single pulse weld (a), CG-HAZ (b) and Rex-zone (c) of double pulse weld, with prior austenite grain boundaries shown in black lines. Misorientation angle distribution of three zone (d)

**Figure 6** shows the inverse pole figure maps and misorientation distribution of CG-HAZs and Rex-zone of the two welds. Prior austenite grain boundaries have been shown in bold black line. As illustrated, finer structure of prior austenite grains is formed in the CG-HAZ of double pulse weld. Misorientation distribution reveals that the fraction of low angle grain boundaries is higher in the CG-HAZ of the single pulse weld compared to that of the corresponding area of the double pulse weld. In contrast, the CG-HAZ of the double pulse weld shows the strongest peak at the high-angle grain boundary range ( $> 47^\circ$ ) and the smallest fraction of low angle grain boundaries. Furthermore, the Rex-zone of the double pulse weld is composed of a microstructure with a high fraction of low-angle grain boundaries and low fraction of high-angle grain boundaries.

Considering K-S orientation relationship between austenite and martensite phase, the variants belonging to different Bain groups are coloured in different hue in **Figure 7a-c**. White and black lines are imposed to the maps indicating the low-angle ( $5 - 15^\circ$ ) and high-angle ( $> 15^\circ$ ) grain boundaries, respectively. Prior austenite grain boundaries are shown in bold black lines. The colour coding applies to each prior austenite grain separately. As it can be seen, variants that belong to different Bain groups keep high misorientation angle in between, whereas variants within one Bain group have a low misorientation angle. Furthermore, the density of low angle grain boundaries (white lines) is higher in the CG-HAZ of single pulse and Rex-zone of double pulse weld as opposed to the CG-HAZ of double pulse weld. Obviously, much finer Bain groups are formed in the CG-HAZ of double pulse weld compared to the CG-HAZ of single pulse and the Rex-zone of the double pulse weld. It is clear that the thermal cycle of welding in the CG-HAZ of single pulse and Rex-zone of double pulse leads to the formation of a structure that shows stronger variant selection as the dominant intervariant boundaries are those belonging to the same Bain group. On the contrary, blocks of martensite in the CG-HAZ of double pulse weld are misorientated with high-angle boundaries as the most of variants belong to different Bain groups.

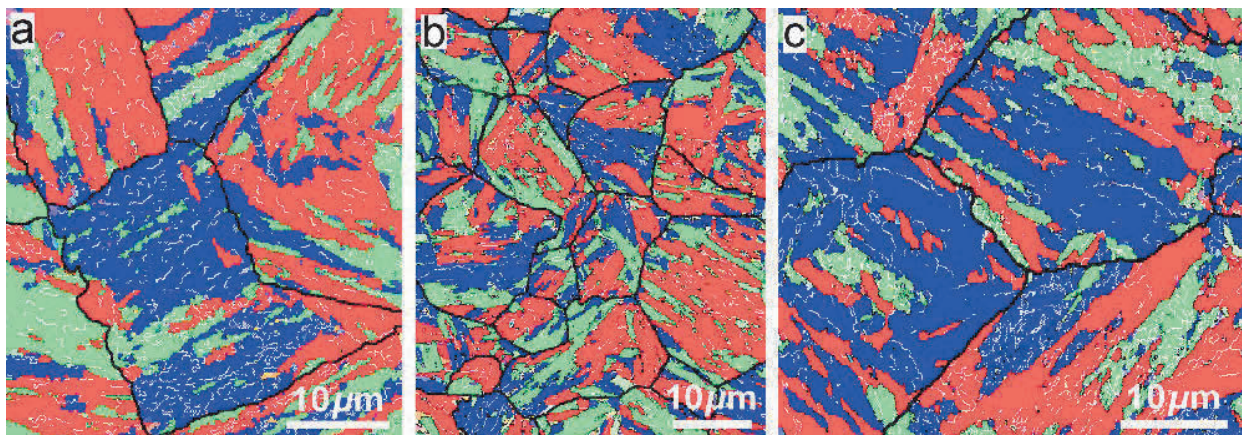


**Figure 7** Bain maps of martensite in CG-HAZ of single pulse weld (a), CG-HAZ (b) and Rex-zone (c) of double pulse weld. White lines indicate low angle ( $5-15^\circ$ ) and black lines are high angle ( $> 15^\circ$ ) boundaries. Prior austenite grain boundaries are shown in bold black lines.

The microstructural characteristics and fracture behaviour of the resistance spot welded DP1000 steel samples can be summarized as follows. Both welds fail in pull-out failure mode. However, in the single pulse weld, failure occurs in CG-HAZ, whereas in the case of double pulse weld, on one side of the weld, crack propagates small distance into the Rex-zone and then is deflected to the CG-HAZ. Rex-zone has coarse structure of Bain groups and low fraction of high-angle grain boundaries. However, this area is thick enough and contains reasonable number of equiaxed prior austenite grains containing packets and Bain groups that are effective in arresting the crack propagation. Thus, cracks are supposed to deflect towards CG-HAZ since it is forced to cross over several equiaxed prior austenite grains in the Rex-zone. Prior austenite grains are finer at the CG-HAZ of double pulse weld and lead to smaller packets of martensite. Besides, variant pairing in this zone

results in the evolution of martensitic microstructure with finer Bain groups. On the other side, failure occurs in the severely softened SC-HAZ which results in the reduction in stress concentration at the weld edge during cross-tension test.

#### 4. CONCLUSION

The effects of welding parameters on the cross-tension strength, failure behaviour and microstructural evolution of DP1000 steel were investigated. Two RSW processes with single and double pulse current were applied. Maximum load increases from 9.2 kN for single pulse processed weld to 11.7 kN for double pulse processed one. The absorbed energy of the single pulse welded sample at maximum load is 55.3 J. This value rises to 75.2 J with applying the second pulse. Besides, double pulse welding leads to more pronounced softening at the SC-HAZ.

It was found that the weld scheme strongly affects the crystallographic features of martensite phase that forms at different weld zones. Grain- boundary characterization shows that a low fraction of high-angle grain boundaries and coarser structure of Bain groups are formed in the Rex-zone of double pulse welds. Finer structure of prior austenite grains, martensite packets and Bain groups are formed in the CG-HAZ of double pulse weld. Better mechanical properties of double pulse weld can be attributed to several softening of SC-HAZ, and to the formation of thick Rex-zone with equiaxed structure of prior austenite grains and fine structure of high-angle Bain groups in CG-HAZ.

#### REFERENCES

- [1] BALUCH, N., UDIN, Z.M., ABDULLAH, C.S. Advanced high strength steel in auto industry: an Overview. *Engineering. Technology & Applied Science Research*, 2014, vol. 4, pp. 686-689.
- [2] TUMULURU, M.D., Resistance spot welding of coated high-strength dual-phase steels. *Welding Journal*, 2006, vol. 85, no. 8, pp. 31-37.
- [3] POURANVARI, M., MARASHI, S.P.H., MOUSAVIZADEH, S.M. Dissimilar resistance spot welding of DP600 dual phase and AISI 1008 low carbon steels: correlation between weld microstructure and mechanical properties. *Ironmaking & Steelmaking*, 2011, vol. 38, no. 6, pp. 471-480.
- [4] DANCETTE, S., FABRÈGUE, D., FABRÈGUE, V., MERLIN, J., DUPUY, T., BOUZEKRI, M. Experimental and modeling investigation of the failure resistance of Advanced High Strength Steels spot welds. *Engineering Fracture Mechanics*, 2011, vol. 78, no. 10, pp. 2259-2272.
- [5] SAWANISHI, C., OGURA, T., TANIGUCHI, K. Mechanical properties and microstructures of resistance spot welded DP980 steel joints using pulsed current pattern. *Science and Technology of Welding and Joining*, 2014, vol.19, no. 1, pp. 52-59.
- [6] JONAS, J.J. Effect of austenite recrystallization on toughness of pipeline steels. *Materials Science Forum*, 2013, vol. 753, pp. 546-553.
- [7] ANDERSON, T. L. *Fracture Mechanics: Fundamentals and Applications*. 3rd ed. London: CRC Press, 2005. 249 p.
- [8] YOU, Y., SHANG, C., WENJIN, N., Subramanian, S. Investigation on the microstructure and toughness of coarse grained heat affected zone in X-100 multi-phase pipeline steel with high Nb content. *Materials Science and Engineering A*, 2012, vol. 558, pp. 692-701.